Fast scanning method for one-dimensional surface profile measurement by detecting angular deflection of a laser beam

Ryo Shinozaki, Osami Sasaki, and Takamasa Suzuki

A fast scanning method for one-dimensional surface profile measurement is proposed. The profile is measured by integration of a slope distribution of the surface obtained from angular deflection of a scanning laser beam. A scanning optical system that consists principally of a spherical concave mirror and a rotating scanner mirror has reasonably low cost and is insensitive to mechanical vibration because of its high-speed scanning, of the order of milliseconds. A surface profile of a polygonal mirror along a 5-mm width was measured with the scanning method and with an interferometer. The root-mean-square difference between the two measured results is 0.98 nm. © 2004 Optical Society of America

OCIS codes: 120.2830, 120.3940, 120.4640, 120.5800, 120.6650.

1. Introduction

In the development of high-precision technology for surface processing, the control and inspection of surface profiles during manufacturing are important, and in-process 100% inspection of products should be carried out to prevent the shipment of defective products. In general, interferometers or instruments made by the stylus method have been used for inspections. However, these instruments need a specialized measurement room because they are vulnerable to mechanical vibration. Therefore in-process 100% inspection cannot be expected as long as these measurement instruments are used.

We describe a method of one-dimensional surface profile measurement by integrating a slope distribution that we obtain by detecting angular deflection of a scanning laser beam. Measurements of slope distribution have already been made; e.g., Smolka and Caudell[1] translated a test object for measuring a slope distribution. Takacs *et al.*[2] and Weingärtner *et al.*[3] translated an optical system and took into consideration the influences of a mechanical system. Since they used a mechanical traverser for the translation of the test object or the translation of the optical system, the translating speed was not sufficient to make the measurement insensible to vibration.

In this paper a scanning method with high speed is proposed. This scanning method is insensitive to vibration because the high measurement speed is of the order of milliseconds. In addition, the optical system possesses a measurement accuracy of the order of nanometers. Therefore it is possible to apply the scanning method to an in-process automatic profile inspection system for the manufacture of precision products.

First, the basic scheme for measuring a one-dimensional profile from a slope distribution of a test surface by detecting angular deflection of a laser beam probing the surface is described in Section 2. The concept of the slope measurement is same as that proposed by Evans.[4] Second, it is shown that an optical system constructed from a spherical concave mirror and a rotating scanner mirror can scan a probing beam at high speed. The optical system is nonaberrational and achromatic. However, some modifications to the arrangement of optical components are required for a test object to be inserted into the optical system for measurement of the one-dimensional surface profile. After the sequential modifications, a practical optical system is determined, as described in Section 3. These modifications cause deviations from the ideal deflection of the laser beam. We analyze the deviations in Section 4 to make clear the characteristics of the optical sys-

R. Shinozaki is with Core System Company, Ltd., 2-2 Nakajima 2, Nagaoka-shi 940-0094, Japan. O. Sasaki (osami@eng.niigata-u.ac.jp) and T. Suzuki are with the Faculty of Engineering, Niigata University, 8050 Ikarashi 2, Niigata-shi 950-2181, Japan.

Received 3 January 2004; revised manuscript received 22 April 2004; accepted 27 April 2004.

0003-6935/04/214157-07$15.00/0

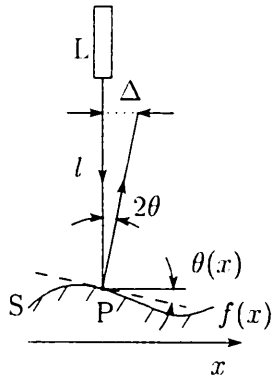

Fig. 1. Basic schematic for measurement of a one-dimensional surface profile by detection of angular deflection.

tem. The effects of a positioning error of the test surface are analyzed in Section 5. Third, the quantitative influence of the errors in the experimental setup is calculated in Section 6. Finally, in Section 7 we describe a one-dimensional surface profile measurement that is carried out by this scanning method without a vibration isolator in the setup. The measured result is compared with the profile obtained by an interferometer to show the usefulness of the scanning method.

2. Basic Scheme for Measurement

A basic schematic of one-dimensional surface profile measurement by detection of angular deflection is shown in Fig. 1. A beam emitted from light source L is scanned on sample surface S. Let the x axis be the scanning direction, which is perpendicular to the incident beam. The surface profile and the slope of the surface along the x-axis direction are expressed by $f(x)$ and $\theta(x)$, respectively, as shown in Fig. 1. If $\theta \ll 1$, the differential of $f(x)$ is given by

$$\frac{df(x)}{dx} = \tan \theta(x) \sim \theta(x). \tag{1}$$

Now the beam is incident onto point P on the surface. The reflected beam deviates from the incident beam by angle 2θ. We find this angle 2θ by measuring beam deflection $\Delta = 2\theta l$ at distance l from point P. Carrying out the same measurement of many points on the surface, we obtain a distribution of deflection $\Delta(x)$. Integration of distribution $\Delta(x)$ and expression (1) gives the one-dimensional surface profile $f(x)$ as follows:

$$\frac{1}{2l}\int \Delta(x)dx = \int \theta(x)dx = f(x). \tag{2}$$

We make use of a photosensor such as a position-sensing detector (PSD) to make the measurement of the deflection $\Delta(x)$. Because the output of the sensor is proportional to the position of the beam spot on the sensor, we have to determine proportionality constant α by comparing a measured surface profile with a known surface profile.

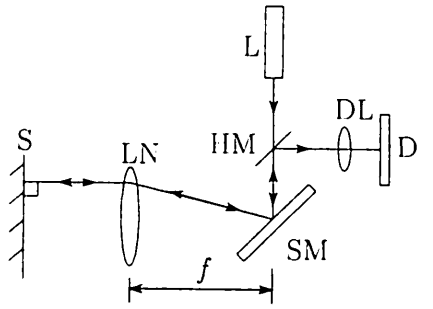

Fig. 2. Optical system for scanning a beam by use of lens LN and scanner mirror SM.

3. Optical System

To carry out a high-speed measurement of distribution of deflection $\Delta(x)$ with the basic scheme shown in Section 2 we must scan the beam spot along the surface at a high speed, and the reflected beam must reach a PSD.

For this measurement the optical system shown in Fig. 2 is considered. The beam emitted from light source L is incident upon a rotating scanner mirror, SM. As scanner mirror SM is placed at focal distance f of lens LN, the beam reflected from the scanner mirror is incident perpendicularly onto sample surface S, which is parallel to lens LN. If surface S is flat plane, the beam reflected from it retraces the incident beam's path precisely. To make the reflected beam incident onto position-sensing detector D and measure the distribution of deflection, we insert half-mirror HM between light source L and scanner mirror SM. If surface S is not flat and has a slope θ, deflection $\Delta = f\theta$ appears on the focal plane of lens LN. Deflection Δ is imaged onto detector D by lens DL. To carry out an accurate beam scan and measurement, we need a lens whose aberration is highly compensated. Because lens LN would become expensive under these conditions, another optical system must be considered.

In this paper the optical system shown in Fig. 3, which makes use of a spherical concave mirror instead of a lens, is proposed. The rotation axis of scanner mirror SM coincides with the center of cur-

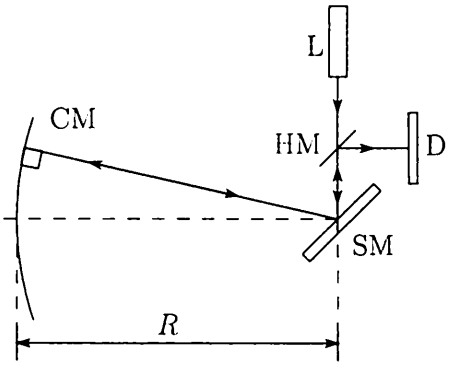

Fig. 3. Optical system for scanning a beam by use of spherical concave mirror CM and scanner mirror SM, where R is the radius of curvature of the concave mirror.

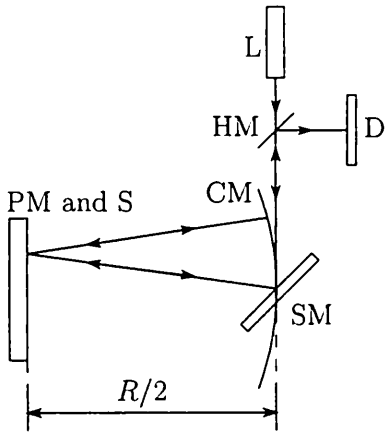

Fig. 4. Introduction of plane mirror and sample surface S into Fig. 3. The PM and the S are put into incident path SM–CM and reflected path CM–SM, respectively.

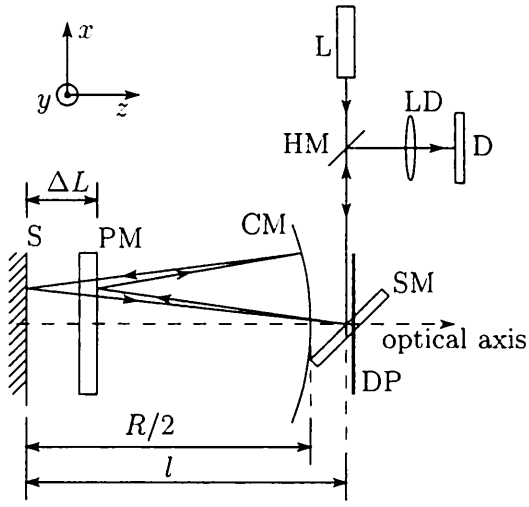

Fig. 5. Separation of sample surface S and plane mirror PM in Fig. 4. S is detached from the PM by ΔL, with the distance between CM and S maintained at $R/2$.

vature of spherical concave mirror CM, where R is the radius of curvature of mirror CM. The beam reflected from the scanner mirror is incident perpendicularly onto concave mirror CM, and the beam reflected from it retraces the path of the incident beam precisely. Hence the position of the beam spot on detector D is constant, independently of the rotation angle of the scanner mirror. The optical system is reasonably low cost because it is free of spherical aberration and is achromatic without the need for optical compensation.

In this optical system one must consider where sample surface S should be put to produce deflection Δ on the detector. Figure 4 shows that plane mirror PM and sample surface S are put into the incident path SM–CM and the reflected path CM–SM, respectively. The beam reflected from scanner mirror SM is incident onto concave mirror CM through plane mirror PM. The beam reflected from concave mirror CM is incident onto scanner mirror SM through surface S. The rotation of scanner mirror SM makes the beam spot move on surface S. We define L_i = |SM–PM–CM| and L_r = |CM–S–SM| as the path lengths of the incident beam and of the reflected beam, respectively. The condition $L_i = L_r = R$ provides a nonaberrational optical system for the scanning. Moreover, it provides maximization of lateral resolution in the scanning because the distance between concave mirror CM and surface S is $R/2$.

However, in practice it is impossible to use the arrangement shown in Fig. 4. Therefore we must consider an arrangement of plane mirror PM, surface S, and concave mirror CM. The arrangement in the z–x plane is shown in Fig. 5, where a Cartesian-coordinate system is defined. The optical axis is the z axis. Concave mirror CM and surface S move away from scanner mirror SM along the optical axis, keeping the distance at $R/2$. Then plane mirror PM is detached from surface S by ΔL along the optical axis. The beam spot on surface S is scanned parallel to the x axis. Because the condition $L_i = L_r = R$ is not satisfied in Fig. 5, the beam reflected from surface S does not return to the original point on scanner mirror SM from which the beam goes out, even if surface S is a flat plane. This displacement of the beam spot can be minimum on an x–y plane that contains the rotation axis of scanner mirror SM if a condition for ΔL given in Subsection 4.A below is satisfied. We call the x–y plane the detecting plane, DP. This slight displacement of the beam spot on detecting plane DP is the spherical aberration of concave mirror CM. Its influence on the measurement is discussed in Section 4.A below. Deflection Δ that appears on plane DP is imaged onto detector D by lens DL. Because the distance between the probing beam spot on surface S and plane DP varies with the rotation angle of scanner mirror SM, deflection Δ is not exactly equal to $2l\theta$, where l is the distance between surface S and plane DP. This deflection is discussed in Subsection 4.B below.

Because all beam paths are in the z–x plane in Fig. 5 and concave mirror CM and plane mirror PM intercept the traveling beam, it is still not possible to use the arrangement in practice. A possible arrangement of optical components is shown in Fig. 6. Rectangular concave mirror CM is displaced in the y-axis direction such that it does not intercept beam path SM–PM. Beam path PM–CM is inclined toward the y-axis direction; it gives a rotation to plane mirror PM such that the beam reflected from PM reaches concave mirror CM. By also giving a rotation to the concave mirror, plane mirror PM does not intercept beam path CM–S. Although beam path S–SM is detached from beam path SM–PM, the two paths becomes parallel to each other by giving a rotation to surface S. In these arrangements the track of the beam spot probing surface S is deflected from a straight line, as discussed in Subsection 4.C below. Fine tuning of the beam spot radius on surface S is performed by lens FL.

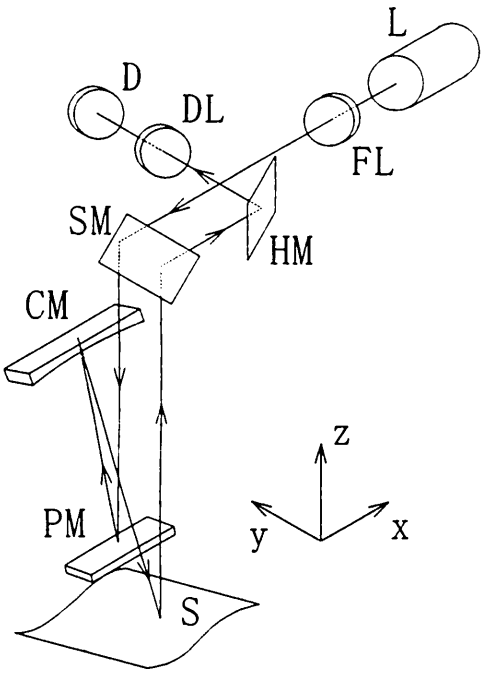

Fig. 6. Optical system modified from Fig. 5. CM is given a displacement and a rotation. PM and S are given different rotations. Beam paths PM–CM and CM–S are inclined toward the y direction.

4. Characteristics of the Optical System

A. Spherical Aberration of the Concave Mirror

Denoting beam path lengths L_i and L_r on the optical axis in Fig. 5 by L_{0i} and L_{0r}, respectively, we have relation

$$L_{0r} - L_{0i} = 2\Delta L. \tag{3}$$

For the measurement of deflection Δ, the condition that L_{0i} and L_{0r} are the conjugate distance of concave mirror CM:

$$\frac{1}{L_{0i}} + \frac{1}{L_{0r}} = \frac{2}{R}, \tag{4}$$

is used. To derive the influence of Eq. (3) on the measurement, we simplify Fig. 5 and change it to Fig. 7. The center of curvature of concave mirror CM is at origin O of the z–x plane. The radius of curvature R of the concave mirror is 1, so the intersection of concave mirror CM and the z axis is B(1, 0). The beam emitted from the scanner mirror whose rotation axis is at point A(d, 0) is incident onto point C on concave mirror CM, which corresponds to the beam path SM–PM–CM in Fig. 5, excluding plane mirror PM. An angle formed by the incident beam's path and the z axis is denoted φ. As the angle varies with the rotation angle of the scanner mirror, we call φ a scanning angle.

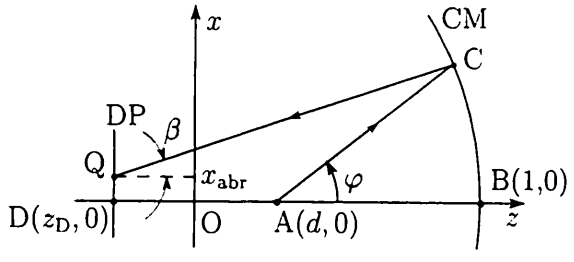

Fig. 7. Displacement of the beam spot on detecting plane DP by the aberration of spherical concave mirror CM when sample surface S is flat. The center of curvature of CM is at origin O of a Cartesian-coordinate system. Rotation axis A of scanner mirror SM and DP is placed at conjugate points of CM.

The beam reflected from point C is incident onto point Q on detecting plane DP, which corresponds to beam path CM–S–DP in Fig. 5, excluding sample surface S. This situation is equivalent to measuring a flat plane. From the relation $L_{0r} > R > L_{0i}$, which is derived from Eqs. (3) and (4), the z coordinate of the rotation axis of scanner mirror SM is $0 < d \ll 1$, and $L_{0i} = 1 - d$. Assuming that the coordinate of the center of detecting plane DP is $D(z_D, 0)$, we have $L_{0r} = 1 - z_D$ and derive

$$z_D = -d/(1 - 2d) < 0 \tag{5}$$

from Eq. (4). Beam spot position Q on detecting plane DP varies with scanning angle φ. The displacement of beam spot Q from point D is obtained from the spherical aberration[5] of concave mirror CM. The displacement is given by

$$x_{abr} = -d^2\varphi^3, \tag{6}$$

where $\varphi \ll 1$. Incident angle β formed by reflected beam CQ and the z axis is slightly different from scanning angle φ. It is given by

$$\beta = (1 - 2d)\varphi. \tag{7}$$

A relation between ΔL and d is derived from Eq. (3) and inequality (5), as follows:

$$2\Delta L = -z_D + d \sim 2d. \tag{8}$$

Therefore, from Eqs. (6) and (8), the influence of the aberration on the measurement is limited by both distance ΔL between plane mirror PM and sample surface S and a maximum of scanning angle φ.

B. Deflection of the Beam on the Detecting Plane

Figure 8 shows a situation in which sample surface S is inserted in Fig. 7 at a distance l from detecting plane DP. Point P on surface S is probed now. If surface S is a flat plane, the beam reflected from concave mirror CM goes straight and reaches point Q on detecting plane DP, as indicated by the longest dashed line PQ in the figure. If the slope at point P is θ, the reflected beam is given a change of 2θ in the traveling direction and reaches point Q′ on plane DP. Then the angle formed by the reflected beam and the z axis is $2\theta + \beta$. From Fig. 8, the x coordinate of beam spot Q′ on plane DP is given by

$$x_\theta = l \tan \beta - l \tan(2\theta + \beta) + x_{abr}. \tag{9}$$

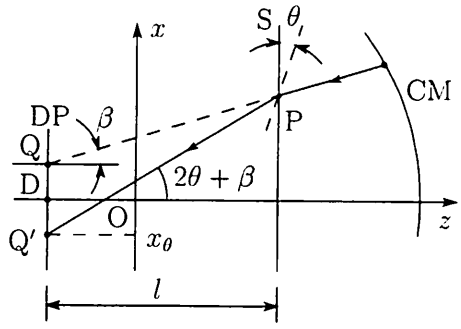

Fig. 8. Deflection of the beam spot on detecting plane DP. Sample surface S is inserted into beam path CM–DP. The traveling direction of the reflected beam is changed at point P owing to the slope θ of surface S.

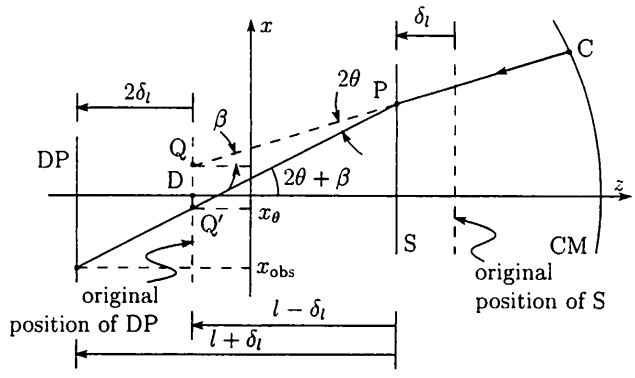

Fig. 9. Effect of positioning error of sample surface S. The position of S is shifted by δ_l.

where x_{abr} is the aberration given by Eq. (6). We expand Eq. (9) in the lowest order of φ, d, and θ; using Eq. (7), we obtain

$$x_\theta = -2l\theta - 2l\theta\varphi^2 + x_{abr}, \tag{10}$$

where $\theta \ll 1$, $\varphi \ll 1$, and $d \ll l$. The first term of Eq. (10) is what we need to measure the slope distribution of the sample surface. The second term is caused by the fact that the distance between point P and detecting plane DP varies with scanning angle φ. Its influence on the measurement is ignored if maximum scanning angle φ_{max} is limited, as shown in Subsection 6.B below.

C. Track of the Beam Spot Probing the Sample Surface

The incident beam's path and the reflected beam's path are not on the same plane in the optical system shown in Fig. 6, so the beam spot's track probing the sample surface is deflected from a straight line. Because deriving an equation for the deflection in the track of the beam spot is rather complicated and is not so important here, only the resultant equation is shown below.

It is assumed that an angle formed by beam paths PM–CM and CM–S in Fig. 6 is 2γ. Then the deflection from a straight line in the track of the beam spot is given by $\varphi^2 R\gamma$. If the deflection is less than beam spot diameter w on the sample surface, the beam spot's track on the surface is regarded as a straight line. This condition is given by

$$\varphi^2 R\gamma < w. \tag{11}$$

5. Effect of the Positioning Error of the Sample

The influence on the measurement of the positioning error of the sample's surface is discussed in this section.

It is assumed that sample surface S shifts by δ_l in the direction of the z axis in Fig. 5. Then Fig. 8 changes to Fig. 9, where the distance between surface S and detecting plane DP is $l + \delta_l$. The beam reflected from concave mirror CM reaches point P on surface S, which shifts by δ_l from its original position. The beam reflected at point P is incident onto detecting plane DP, which shifts by $2\delta_l$ from its original position. Replacing l with $l - \delta_l$ in Eq. (9), we derive the x coordinate x_θ of point Q′ as

$$x_\theta = (l - \delta_l)\tan\beta - (l - \delta_l)\tan(2\theta + \beta) + x_{abr}. \tag{12}$$

Displacement x_{obs} of the beam spot on the shifted detecting plane DP is equal to $x_\theta - 2\delta_l \tan(2\theta + \beta)$. Therefore, if $\delta_l \ll 1$ and we expand displacement x_{obs} in the lowest order, we obtain

$$x_{obs} = -2(l + \delta_l)\theta - 2(l + \delta_l)\theta\varphi^2 - d^2\varphi^3 - 2\delta_l\varphi, \tag{13}$$

using Eq. (7). Coefficient $(l + \delta_l)$ of the first and second terms of Eq. (13) is found from the distance between a detecting plane DP and surface S. The fourth term, $2\delta_l\varphi$, contains an error caused by a positioning error of sample surface S. Because this term is a linear function of scanning angle φ that is proportional to the x coordinate of the probing position, the influence of the error on the profile measurement appears as a quadratic function of the x coordinate. If it is necessary to eliminate the error, the quadratic functional component should be subtracted from integral of x_{obs} by the least-squares method.

6. Experimental Setup

The configuration of the experimental setup is described and the error estimation for measuring a surface profile of a polygonal mirror along a 5-mm width is shown in this section.

A. Configuration

The optical system of the setup was the same as shown in Fig. 6. Light source L was a He–Ne laser, and the laser beam emitted from it was collimated 5 mm in half-width by focusing lens FL. Spherical concave mirror CM had an 80-mm diameter, a radius of curvature of $R = 400$ mm, and surface flatness $\lambda/4$. It was cut into a 15 mm × 80 mm strip. The distance between concave mirror CM and surface S was $l = 200$ mm, which was the focal distance of concave mirror CM. In this condition, the half-width of the beam spot diameter on surface S was $w = 30$ μm. Mirrors PM, SM, and HM had $\lambda/10$ surface flatness.

Lens DL with 100-mm focal distance was achromatic. Distance ΔL, almost equal to d between plane mirror PM and sample surface S, was 7 mm.

The PSD was a Hamamatsu Photonics K.K. model S1880 detector. The output current of the PSD is proportional to both the beam spot's position on its surface and the beam's intensity. After the output current of the PSD was converted into a voltage by an operational amplifier, it was divided by a voltage proportional to the beam's intensity to eliminate the dependence of the output current on the beam's intensity. A Burr Brown MPY634 analog divider was used for the division. The output signal of the processing circuit described above was fed to a computer through a 12-bit analog-to-digital converter.

Scanner mirror SM was mounted upon a motor with a 250-rpm rotating speed. The distance between scanner mirror SM and sample surface S was approximately 200 mm, so the scan speed of the beam spot on surface S was 5 mm/ms. Because the measurement time was 1 ms, the setup was insensitive to vibrations lower than 1 kHz. Therefore the experiment could be performed with no vibration isolator.

B. Error Estimation

Because positioning error δ_l of the sample surface could be less than 0.4 mm, the ratio of δ_l to l was 10^{-3}. Therefore we can regard the term $l + \delta_l$ as l in Eq. (13), and a one-dimensional surface profile is obtained from the integral of the first term of Eq. (13).

The second term of Eq. (13) is the error that depends on scanning angle φ. The ratio of the second term to the first term is φ^2. As a surface profile was measured along a 5-mm width, the maximum scanning angle was $\varphi_{max} = 2.5/200 \sim 10^{-2}$. The value of $\varphi_{max}^2 \sim 10^{-4}$ was less than the resolution of the 12-bit analog-to-digital converter. Therefore the second term of Eq. (13) could be ignored.

The third term of Eq. (13) indicates the spherical aberration of the spherical concave mirror. The ratio of the third term to the first term is $[d^2\varphi^3/(2l\theta)]/R$. It was found from measurement with a Veeco Instruments Wyko NT3300 interferometer that the root mean square of the slope distribution of the polygonal mirror was $\theta_{rms} \sim 10^{-4}$. Because $d^2\varphi_{max}^3/(2l\theta_{rms})/R \sim 10^{-6}$, the spherical aberration of the concave mirror could also be ignored.

The fourth term of Eq. (13) caused by the positioning error of the sample is the linear function of φ. The ratio of the fourth term to the first term was $\delta_l\varphi_{max}/(2l\theta_{rms}) \sim 10^{-1}$. As mentioned in Section 5, the influence of the positioning error appears in the integration of Eq. (13) as the quadratic functional component. This error component was derived by a least-squares method and was subtracted from the integration of the output signal of the processing circuit. Moreover, in the condition that sample surface S was not parallel to the x axis, the signal had a constant current that appeared as a linear component in the integration of the signal. This component was eliminated in the same manner as the quadratic component.

We had $\gamma = 5/200$ and $\varphi_{max}^2/R\gamma \sim 0.001$ mm for inequality (11). As $w = 0.03$ mm, inequality (11) was satisfied.

The angular speed of the scanner mirror is constant, but the motion of the beam spot on the sample surface is not constant, as shown by Eq. (7) and Fig. 8. The data were not sampled at a constant interval with respect to the x coordinate. The variation of this spatial sampling interval is estimated here. If the aberration and the slope θ in Fig. 8 are ignored, the x coordinate of the beam spot on surface S is given by $x = l \tan \beta = l \tan[(1 - 2d)\varphi]$. By differentiating x with φ, we have

$$\frac{\partial x}{\partial \varphi} \sim l(1 - 2d) + l\varphi^2, \tag{14}$$

where $d \ll 1$ and $\varphi \ll 1$. As the relative magnitude of the variation in the spatial sampling intervals was $\varphi_{max}^2/(1 - 2d) \sim 10^{-4}$ at most, it was considered that the slope data were sampled at a constant spatial interval.

7. Experimental Tests

A. Measurement of a Standard Plane

Whereas the root mean square of the profile of the polygonal mirror was 3.5 nm, the spherical concave mirror had a surface flatness of $\lambda/4 \sim 160$ nm, and other mirrors had $\lambda/10 \sim 63$ nm. Therefore we could not ignore the influence of surface distortion of the optical components. We estimated this influence by measuring a flat plane as a standard plane that was a square plane mirror with surface flatness $\lambda/20 \sim 32$ nm.

A profile F_{ST}, which indicates the influence of surface distortion of the optical components, was obtained in the following way: (1) The slope data were collected by a computer, and we obtained an integrated value V_s by numerical integration. (2) The quadratic functional component V_q of the integrated value V_s was derived by a least-squares method. (3) We obtained a profile $f_s = V_s - V_q$. (4) As fine components of f_s were not required, profile f_s was smoothed to a width of 0.24 mm, so F_{ST} was obtained.

Profile F_{ST} is shown in Fig. 10. Profile F_{ST} shows distortion of both plane mirror PM and concave mirror CM. To perform the profile measurement with compensation for this distortion, one should subtract profile F_{ST} from a surface profile obtained from steps (1)–(3) of the procedure above for a sample surface.

B. Calibration and Surface Profile Measurement

A surface profile of the polygonal mirror was measured in steps (1)–(3) of the procedure described above. The measured profile is denoted f_{C_l}. It is expected that profile f_{C_l} will be proportional to the true surface profile of the polygonal mirror. To determine this proportionality constant α, we also measured the profile with a Wyko NT3300 interferometer, and we eliminated the quadratic functional component contained in the measured profile

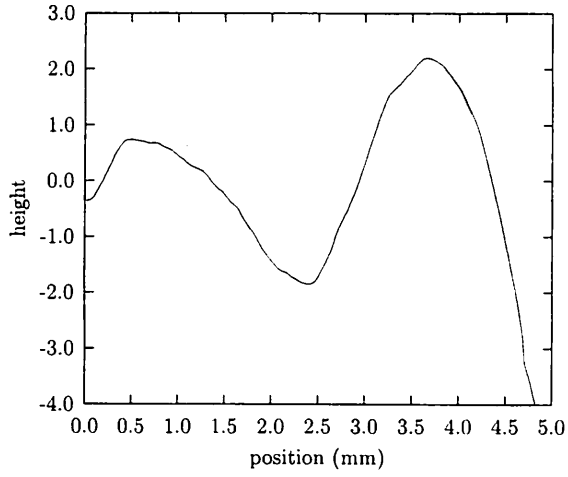

Fig. 10. Profile F_{ST} obtained from measurement of the standard plane with $\lambda/20$. Profile F_{ST} shows the influence of the surface distortion of optical components used in the setup.

to obtain surface profile f_i. We determined constant α by using a minimizing equation

$$\sum_i (f_i - \alpha f_{C_i})^2, \tag{15}$$

where the subscript i means the position of the sample surface. In this experimental setup, constant α was 0.99. Profile αf_{C_i} and f_i are shown in Fig. 11.

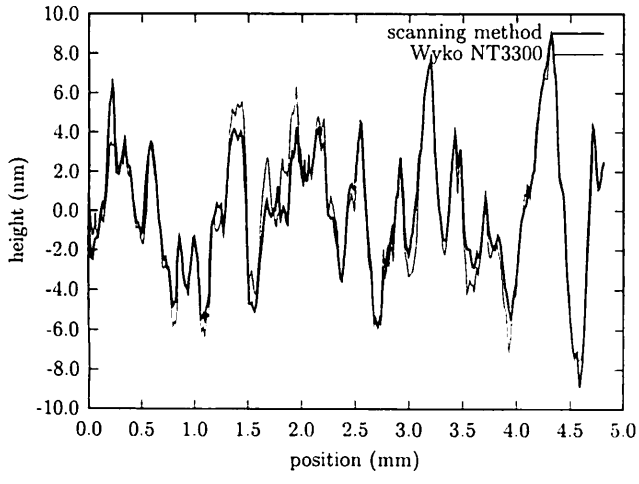

Fig. 11. Measured surface profiles of a polygonal mirror.

The root-mean-square difference between profiles αf_{C_i} and f_i was 0.98 nm.

To investigate the stability of the measurement by this scan method, we repeated this measurement 20 times. The root-mean-square measurement repeatability was 0.31 nm.

8. Conclusions

We have described one-dimensional surface profile measurement by detection of the angular deflection of a fast-scanning laser beam. Because the scanning optical system consists principally of a spherical concave mirror and a rotating scanner mirror, it has a reasonably low cost and is insensitive to vibration because of its high-speed measurement, of the order of milliseconds.

Although the use of the concave mirror ideally offers a nonaberrational and achromatic optical system, the practical optical system finally decided on involved deviations from the ideal deflection of the laser beam. A theoretical analysis of the optical system has made it clear that the influence of the deviations on the surface profile measurement can be ignored in the experimental setup.

A surface profile of a polygonal mirror along a 5-mm width was measured with the setup. The measurement time was 1 ms, and no vibration isolator was needed. Compared with the surface profile measured with a Wyko NT3300 interferometer, the root-mean-square difference between the two measured surface profiles was 0.98 nm.

References

1. F. M. Smolka and T. P. Caudell, "Surface profile measurement and angular deflection monitoring using a scanning laser beam: a noncontact method," Appl. Opt. **17,** 3284–3289 (1978).
2. P. Z. Takacs, S. K. Feng, E. L. Church, S. Qian, and W. Liu, "Long trace profile measurements on cylindrical aspheres," in *Advances in Fabrication and Metrology for Optics and Large Optics*, J. B. Arnold and R. E. Parks, eds., Proc. SPIE **966,** 354–364 (1988).
3. I. Weingärtner, M. Schulz, and C. Elster, "Novel scanning technique for ultraprecise measurement of topography," in *Optical Manufacturing and Testing III*, H. P. Stahl, ed., Proc. SPIE **3782,** 306–317 (1999).
4. J. D. Evans, "Method for approximating the radius of curvature of small concave spherical mirrors using a He–Ne laser," Appl. Opt. **10,** 995–996 (1971).
5. M. V. Klein, *Optics* (Wiley, New York, 1970).